2020 IEEE/RSJ International Conference on Intelligent Robots and Systems (IROS)
October 25-29, 2020, Las Vegas, NV, USA (Virtual)

Design and Implementation of a Haptic Measurement Glove to Create Realistic Human-Telerobot Interactions

Evan Capelle[1], William N. Benson[1], Zachary Anderson[2], Jerry B. Weinberg[2], and Jenna L. Gorlewicz[1]

***Abstract*— Although research indicates that telepresence robots offer a more socially telepresent alternative to conventional forms of remote communication, the lack of touch-based interactions presents challenges for both remote and local users. In order to address these challenges, we have designed and implemented a robotic manipulator emulating a human arm. However, contact interactions like handshakes with a robotic manipulator may feel awkward and unnatural to local users. In this work, we present the design of a wearable haptic measurement glove (HMG) and use it to collect force and inertial data on handshakes in human-human and human-robot interactions in the interest of developing intelligent shared control algorithms for natural, human-like contact interactions in human-robot interactions.**

I. Introduction

Telepresence robots, or telerobots, provide immediate video and audio connection to a remote operator, enhancing the communication capabilities of a video call with an added social telepresence for the operator. Telerobots allow control of the robot's direction (and thus the camera view) and the ability to move within the local environment [1] [2] [3] [4]. This enhanced telepresence has been shown to benefit remote workers in various settings by allowing them to be more available and present to those in the local space, more able to capture and retain attention, and more able to socially engage with their local colleagues [1]. However, current commercial telerobotic platforms lack the capability to accommodate tangible interactions and expressive gestures that are an integral aspect of face-to-face communication. This results in a social experience that falls extremely short, for both local users (those interacting with the telerobotic platform) and remote users (those controlling the telerobot remotely), of having a experience of a shared physical presence [5]. Previous studies have have shown that incorporating a tangible, humanoid limb onto a telerobotic platform can improve engagement and social connectivity, between remote and local users, from the addition of non-verbal communication typically used in face-to-face interactions [6] [7] [8] [9]. In [9], the term "pilot user" denotes the person operating the telerobot whereas we use "remote user" for this paper.

In previous work [10], we designed and implemented a 4-DOF manipulator created specifically for enhancing telerobots that can execute the three primary social behaviors: tangible interactions (e.g handshakes), expressive gestures, and referencing (pointing). The "shoulder" of the manipulator is mounted rigidly with clamps to the main column of the telerobot such that balance is not affected. One area that we found particularly difficult to execute were interactions that require coordination between local and remote users, such as handshakes. These are challenging because they require real-time sensing and control algorithms to respond to a local user's motions with immediate feedback to the remote user to create the sense of a natural interaction. In this work, we explore the complexities of handshakes in both human-human interactions (HHI) and human-robot interactions (HRI). We present a wireless, haptic measurement glove (HMG) that collects force and inertial data on both human-human and human-robot handshakes (Fig. 1), thus enabling comparison of the two. This work is the necessary basis for the development of intelligent shared control algorithms for coordinated gestures in teleprescence to provide remote and local users a responsive social contact interaction.

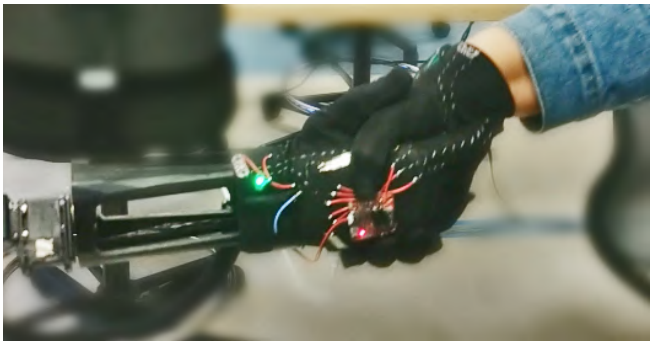

Fig. 1. A participant wearing the HMG shaking hands with the HMG-equipped telerobot.

II. Background

Telerobots, such as the Anybots QB 2.0 (Fig. 2), are frequently used as a means for remote workers to more directly communicate and interact with local colleagues in a workplace [11]. In addition to enhancing the telepresence of remote users, they have been shown to enable more efficient communication and greater social connection between remote and local workers [1]. However, the lack of a haptic communication channel in most commercial telerobots is a notable limitation, as touch is a key component of effective communication [12] [13] [14]. The incorporation of touch into other telecommunication mediums such as audio and video chat systems has been shown to enable superior telepresence compared to telepresence without touch channels

[1]Department of Mechanical and Aerospace Engineering, Saint Louis University, Saint Louis, MO 63103, USA {evan.capelle, william.benson, jenna.gorlewicz}@slu.edu
[2]Department of Computer Science, Southern Illinois University Edwardsville, Edwardsville, IL 62025, USA {zaander, jbweinbe}@siue.edu

Fig. 2. The Anybots QB 2.0 (left) and the modified QB telerobot (right).

[15] [16]. In particular, the study presented in [6] investigated the effects of combining haptic and visual channels by analyzing participants' handshakes with a robotic hand remotely operated by a user displayed on a video screen. The robotic hand was designed to emulate a human hand, capable of emitting heat and imitating human grip force, as well as using urethane gels, urethane sponges, and artificial skin to appear and feel human-like. The results indicated that the combination of visual and haptic channels (i.e. the live video feed and the robotic hand) greatly enhanced the remote user's telepresence compared to the visual channel alone. Such studies support the advantages of haptic communication in telepresence, yet there are several difficulties, in addition to technical complexities, of integrating such capabilities onboard telerobots.

Haptic capabilities are critical for social contact interactions, such as handshakes, fist bumps, and high fives. These interactions are particularly challenging due to their complex nature and the "disconnect" that currently exists haptically between remote and local users. Social contact interactions, particularly handshakes, are ubiquitous in HHI, and are very impactful nonverbal aspects of communication and social interaction; handshakes themselves, so much so that they have been shown to even influence judgements of personality [17]. Several wearable haptic devices have been developed to examine the characteristics of handshakes, some with the goal of translating these characteristics to HRI [18]. A tactile sensing glove (TSG) for measuring properties of human-human handshakes is described in [19], the final design of which contains a total of 20 FSR (force-sensitive resistor)-based sensor blocks distributed in three concentrations on the hand. In addition to having a relatively large footprint, some blocks returned very low outputs in handshake experiments, indicating that these parts of the hand were not actively involved in typical handshakes. A design for another wearable device for measuring handshake characteristics is presented in [18], in which 6 force sensitive resistors (FSRs) are positioned at key points on the bottom, palm, and back of the hand. Also attached to the back of the hand is a 6-DOF inertial sensor, equipped with an accelerometer and a gyroscope. The device was demonstrated to be capable of defining both quantitative and qualitative characteristics of human-human handshakes. While these devices have been shown to successfully capture data on handshake characteristics, they were designed specifically for collecting data on human-human handshakes and do not necessarily account for the potential differences between a human hand and a robotic hand. In order to examine the respective characteristics of handshakes in HHI and HRI, we present a wearable haptic device, the HMG, designed to acquire force and inertial data for both human-human handshakes and human-robot handshakes. Though similar to the device presented in [18] in its use of FSRs and an accelerometer, the HMG has been designed and built to accommodate the need to integrate it into a customized robotic system and with the goal of minimizing sensor and wiring footprints. The HMG also uses a commercial microcontroller that may be programmed to the devices specific needs, enabling it to be used as either a node in a larger robotic system or as a data collection and storage device. Furthermore, while being used for data collection and storage, the HMG is powered by an onboard battery and features a microSDcard for easy data storage and analysis. In this work, we also provide a comparison of handshake data produced by human-human and human-robot interactions, using the HMG. This work sets the stage for future advancements in the design of a robotic manipulator for a telerobot, including a shared control algorithm or haptic feedback system for more natural and human-like contact interactions between telerobots and local users.

III. Current Telerobot System

This work is part of a larger project focused on improving the social connectedness of remote and local users in telepresence interactions. Our current system consists of a modified commercial telerobotic platform - the Anybots QB 2.0 [20] - equipped with a custom robotic manipulator controlled through a virtual reality tracking system (Fig. 2). The initial design and validation of the manipulator were presented in previous work [10]. Recent advancements in the manipulator's design have added a fifth degree of freedom: forearm rotation (Fig. 3). Additionally, the OpenBionics Brunel Hand 2.0, a robust, compact, five-fingered robotic hand, now serves as the manipulator's end effector, replacing the OpenBionics Ada Hand used in the previous iteration. Technical details of the Brunel Hand 2.0 are privided in Table I. The telerobot itself has been modified to feature a larger video screen (Samsung 19" SF350 LED monitor) to better

Fig. 3. The 5-DOF robotic manipulator.

visualize the remote user and a higher quality speaker with external volume control (Elegiant SR100 computer speaker).

Control of the manipulator is achieved through the HTC Vive virtual reality tracking system [21]. The remote user's shoulder position is manually set with a handheld HTC Vive controller while a wearable Vive tracker [22] tracks arm movements. A Manus VR Prime One glove [23] tracks the movements of the user's fingers. The user's movements are translated to motor commands for the manipulator, allowing the user to operate it directly. As such, the manipulator is fully dependent on the remote user, mirroring the remote user's arm and hand movements on the telerobot in real time.

However, this dependence makes contact interactions, such as handshakes, more difficult, as the remote user receives only visual feedback via a camera mounted above the manipulator. Contact interactions are complex and likely require haptic feedback, including speed and applied force from both participants. In the current system, the only data the robot can gather is the motor data: velocity, position, and effort. This data alone cannot provide a complete profile of external contact interactions, which would include force applied on and by the robotic hand, as in a human handshake [19] [18]. In this paper, we present a haptic measurement glove (HMG) to sense and transmit force and inertial information to the robot to enable active motor adjustments in real-time without remote user input. This work sets the stage for a shared control architecture of the manipulator to execute complex, tangible social interactions, such as handshakes in a streamlined, user-friendly way.

IV. Glove Design

A. Constraints

The design constraints of the HMG are dictated by the robotic hand's form and motion, a human hand's form and movement, and the haptic information required for quantifying contact interactions. The goal of the HMG is to acquire necessary sensing information without being obtrusive to the look and feel of the manipulator. Therefore, the glove must fit snugly on the robotic hand without restricting the tendon and spring actuated finger movement. It must also fit comfortably as a one-size-fits-most on human hands. The glove has to accurately collect data and upload it to external storage for processing. It also must be able to send data in real-time to the telerobotic control system. For the glove to be useful in cases not specific to the telerobotic manipulator platform, it must be customizable with the ability to add/remove sensors and edit control software to interface with different robotic systems. Additionally, the glove cannot add significant weight to the manipulator or have a large form-factor so as not to interrupt the anthropomorphic aesthetic of the manipulator. It must also feel comfortable and anthropomorphic to the touch of the local user so as not to interrupt contact interactions.

TABLE I
Technical Specifications

Brunel Hand 2.0		
Mass	***Dimensions***	***Maximum Actuator Force***
332 *g*	198 x 127 x 55 *mm*	45 *N*
FSR 402		
Diameter	***Actuation Force***	***Force Sensitivity Range***
18.28 *mm*	0.1 *N*	0.1-10.0[2] *N*

B. Final Design

The HMG (Fig. 4) consists of a silk glove with force sensitive resistors (FSRs), a slide switch, an LED, a built-in battery, an SD card, and an IMU on a 9-DOF Razor IMU microcontroller. It has 14 total sensing capabilities (5 FSRs + 9 degrees of freedom IMU) and can form-fit to most sized hands, including the Brunel 2.0 Hand. All electrical connections are made with insulated wires and stainless steel conductive thread. The glove is wireless and has a battery life of approximately 18 hours. A SparkFun 9 Degrees-of-Freedom (DOF) Razor IMU [24] is chosen because it contains a built-in inertial measurement unit (IMU), which is used to measure a full motion profile of human and corresponding robotic gestures. This is achieved with a combination of a 3-axis accelerometer, gyroscope, and

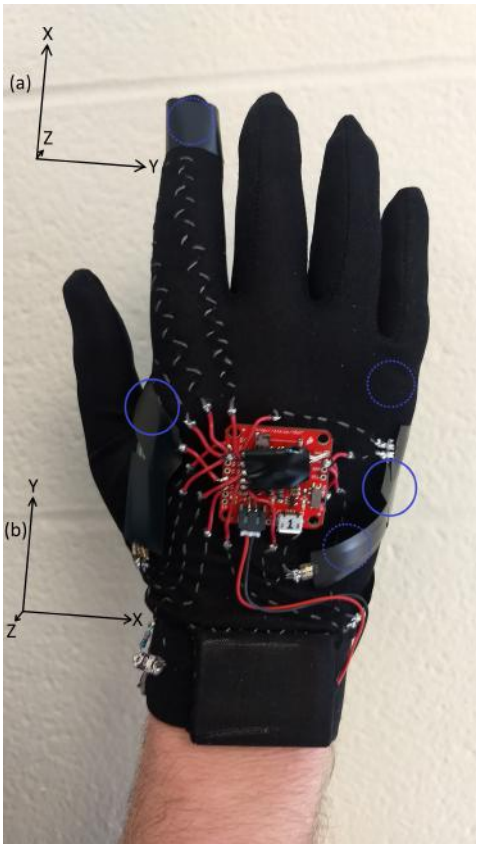

Fig. 4. The HMG components: silk glove base, FSRs (locations circled with dotted lines representing a sensor on the palm side), slide switch, LED, built-in battery, SD card, 9-DoF Razor IMU microcontroller, insulated wires, conductive thread. The orientation of the IMU axes is different for the (a) accelerometer/gyroscope and the (b) magnetometer. In (a), the positive z-axis is in the palm direction. In (b), the positive z-axis points in the dorsal direction.

magnetometer which measure linear acceleration, angular rotation, and orientation respectively. The board has five analog input pins, eight broken out digital I/O pins, and a microUSB port for wired power and data transfer. It runs on and can output 3.3V at 45mA. The Razor IMU board additionally has an SD card slot and a port for an external battery, which enables portable power and portable data storage to create a wireless glove platform. It also maintains a slim profile so as not to interrupt the form and flexibility of the glove.

The base for this design is a black silk liner glove chosen for its strength, sleek design, breathability, and ability to fit most human hands as well as the Brunel 2.0 hand without movement restriction. The wiring is simplified with a combination of conductive thread for flexibility and insulated wire to allow wire crossing and stable connections. Conductive thread is a common wiring method for wearable electronics to maintain a low profile.

FSRs [25] are three layer sensors consisting of a conductive layer, a spacer, and an interdigitating electrode layer. Technical details are provided in Table I. When there is no pressure applied, resistance is at a maximum; applied force causes the conductive layer to connect the interdigitating layer and allow current flow as a variable resistor. The voltage across an FSR is measured by the microcontroller and mapped to an analog value (0-1023). To calibrate the FSRs and convert the analog value to a usable force value in Newtons, an increasing known force is applied to an FSR and a mean analog value is recorded. Linear fit lines ($R > 0.95$) are applied to the resulting analog value vs. known force curve to provide conversion equations. Connected to the FSR input pins are 10-k pull-down resistors to prevent floating ground noise. Five FSRs are placed on points of the glove determined by preliminary benchtop validation tests to have concentrated contact during a handshake. These points are on (1) the tip of the index finger, (2) the heel of the ulnar side of the palm, (3) the base knuckle of the little finger on the ulnar side of the palm, (4) the middle of ulnar side of the hand between the palm and the back of the hand, and (5) the radial side of the base knuckle of the index finger. The FSR on the tip of the index is Interlink Electronics FSR Model 402S, which has a short lead and a 8mm diameter active area. This was chosen because the tip of the index does not provide enough area to mount a regular FSR. The rest of the FSRs are Interlink Electronics FSR Model 400 that has a 12.7mm diameter active area. FSRs are held in place by an adhesive layer on one end and by a sewn wiring connection on the other as well as covered by electrical tape to prevent edges from being pulled up during contact interactions.

A small slider switch and an LED from the Arduino LilyPad line of wearable electronic components are added to the glove to control data logging. The full wiring diagram is provided in Fig. 5. When the switch is turned on, the Razor IMU begins recording data from the FSRs and the IMU onto the SD card and the LED turns on to indicate that recording is successfully occurring. When the switch is turned off, the recording stops, and a new file is created automatically when the switch is turned on again to separate trials. Two identical gloves were made to provide information on both hands involved in a handshake.

V. Methods

Toward comparing HHI and HRI in handshakes, a two part experiment was conducted. Using the HMG described above, we collected force and inertial data on handshakes between (1) subjects and a confederate and (2) between subjects and the confederate-operated telerobot in order to identify quantitative and qualitative characteristics of each and to compare the execution of handshakes between the two scenarios. A handshake was the chosen contact interaction for this study because it is more complex than other contact interactions such as high-fives and fist bumps and requires a degree of tactile feedback to which the remote user does not have access. A total of 10 subjects participated in this study, each in 20 trials total. The study, which was approved by the university's Institutional Review Board, is comprised of two parts: 1) collecting data from human-human handshakes to quantify desired, target interaction profiles for a shared-control or remote haptic feedback architecture; and 2) collecting data from human-robot handshakes to determine the current performance of the robot when a remote user is controlling the interaction. During the HHI trials, two subjects, a participant and a confederate, are equipped with a HMG and instructed to stand at arm's length. Each subject slides the switch on the glove and observes the green confirmation LED to begin the data recording, returns their arm to idle position, carries out a handshake, and returns their arm to idle before sliding the switch to off. This is repeated 10 times for 10 separate pairs of subjects to record 100 total human-human handshakes. For the HRI trials, participants are instructed to perform the same steps as in the human-human stage. Each participant stands at arm's length in front of the robot, slides the switch on the glove and observes the green confirmation LED to begin the recording, returns their arm to idle position, carries out a handshake, and returns their arm to idle before sliding the switch to off. Simultaneously, the experimental coordinator begins the data recording on the glove on the robot. A confederate remote user operates the manipulator

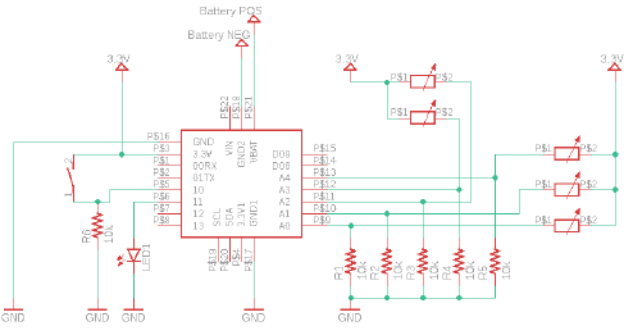

Fig. 5. The circuit diagram for the HMG is centered on the Razor IMU board. FSRs represented as variable resistors have pull down resistors to prevent floating ground noise. The power is provided by a battery and delivered with 3.3V.

to perform a handshake with the participant, then returns the manipulator to an idle position. The coordinator then slides the switch on the robot's glove off. This is repeated 10 times for 10 participants for 100 total recorded human-robot handshakes.

For both HHI and HRI trials, participants are instructed to perform a handshake that feels natural to allow natural subconscious reactions to each handshake. Therefore, the handshakes are performed and terminated based on natural ques such as loosening grip or slowing movement. Since the remote user during HRI does not receive force feedback, the hypothesis of this experiment is a significant difference between HHI and HRI handshakes for metrics quantified by the HMG.

A. Data Analysis Metrics

Handshakes can be categorized quantitatively by five factors: vigor/energy, duration, number of up and down "pulses," firmness/grip strength, and completeness of grip [17]. Vigor, duration, and pulse number can be determined from the accelerometer, gyroscope, and magnetometer data collected in this work although the accelerometer is used primarily to quantify these characteristics because its data values are the most prominent and consistent as described in Section VI. Completeness of grip, firmness, and duration can be computed from the FSR data. These five factors of handshakes are used because they require both tactile and kinesthetic quantification, which tests the full haptic capabilities of the HMG.

Data collected during trials include force data from the FSRs and acceleration, gyroscopic, and orientation data from the IMU. With these, a profile of each handshake is generated. Data on handshake duration, waveform amplitude, number of waveform peaks, number of sensors activated, and force magnitude of activated sensors are recorded for each trial and averaged, and a t-test is performed on each set (HHI vs. HRI) to determine significant differences. Average contact interaction duration is recorded from the first point of hand contact to the full grip release. Additionally, human handshakes can be parsed into stages as demonstrated by [18]. Trends in the handshake stages as well as quantitative data from the five handshake categories are evaluated and compared between HHI and HRI.

VI. Results

We now present our results from the comparative study, detailing our findings with respect to the 5 categories characteristic of handshakes as well as our observations of the overall handshake profiles and their distinct stages.

In interpreting the results, it is important to note that the positive y-axes for the accelerometer and gyroscope points down (in the direction of gravity) when the arm is extended parallel to the ground with the palm of the hand perpendicular to the ground during a normal handshake. The axes orientation for the IMU in relation to the HMG is provided in Fig. 4. A representative time-plot of 3-axis linear accelerations for human-human and human-robot handshakes are shown in Fig. 6 for context as the results are discussed. A video example comparing HHI and HRI handshakes is provided in [26].

A. Handshake Stages

In contrast to the four stages described in [18], our results showed five stages of handshakes for both HHI and HRI. Stage 1 is between the start of the data recording and the initial contact, during which participants in the interaction raise their arms from idle position. During this approach stage, the hand rotates around the z-axis according to gyroscopic data, and the hand experiences relatively constant linear accelerations (Fig. 6). The orientation changes according to the magnetometer data (in which the z-axis is perpendicular to the magnetic north direction so that magnetic pull only changes along the x-axis and y-axis). There is no FSR data for this stage because no physical contact is made. Stage 5 is between the termination of physical contact at the end of the handshake and the end of the recording during which the participants lower their arms. Stage 5 mirrors stage 1. It involves rotation around the z-axis corresponding to an orientation change. Linear acceleration is relatively constant, and there is no FSR data as the hands return to idle position.

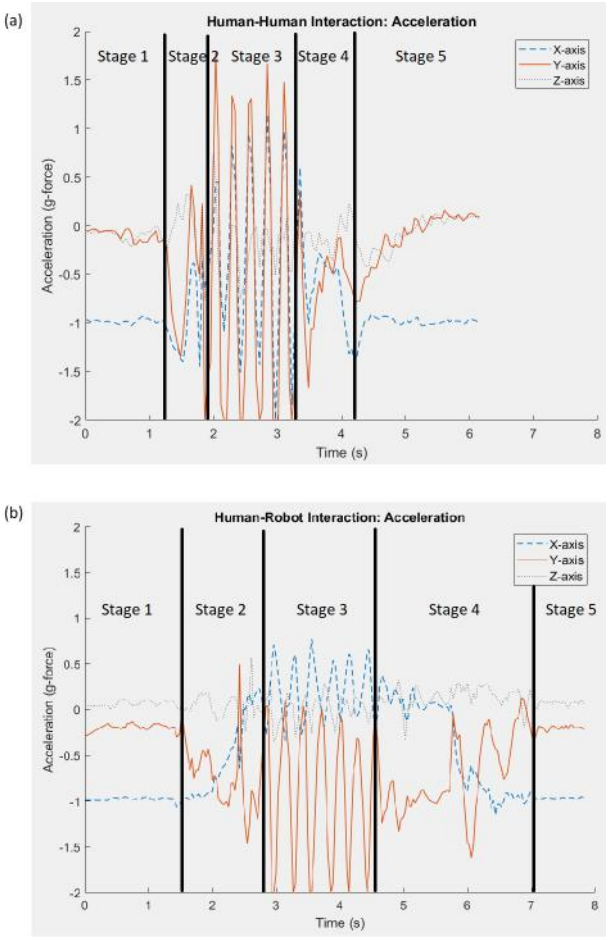

Fig. 6. Representative time-plots of 3-axis linear acceleration for (a) human-human and (b) human-robot handshakes are divided into five stages. The z-axis plots are less visible to avoid crowding of higher amplitude data.

Stages 2, 3, and 4 characterize the contact portions of the interactions. In stage 2, participants make physical contact and start their handshake movement while subconsciously determining how the handshake will proceed. Stage 3 is the main stage of the handshake during which both participants are comfortable with each other's desired handshake and have compromised, creating a steady, consistent waveform of up and down motion. Stage 4 is the period between when one or both of the participants want to end the handshake and when they actually terminate contact. The steady waveform of stage 3 is broken to initialize stage 4.

For both the HHI and HRI handshakes, stages 1 and 5 exhibit relatively constant accelerations across the 3 axes with low magnitude fluctuations. Stages 2 and 4 consist of highly unsteady data which varied from trial to trial throughout the study. Stage 3 depicts a relatively steady waveform for both the x-axis and y-axis. Movement along the y-axis is vertical movement during a handshake, movement along the x-axis is horizontal movement toward or away from the participants' bodies, and movement along the z-axis is side to side movement across the front of participants. The y-axis waveform exhibits a larger amplitude than the x-axis waveform. In this stage, the z-axis also reveals a low-amplitude waveform in phase with the y-axis waveform. This shows that prominent movement during stage 3 is vertical while corresponding small horizontal movements along the x-axis and z-axis occur. The similarities and differences observed in each stage are discussed in more detail in Section VII.

B. Handshake Metrics

We now further analyze stages 2, 3, and 4 of the HHI and HRI handshakes in the context of the 5 characteristics of handshakes [17]. Note that the null hypothesis for all of the statistical tests states that there is no significant difference between HRI and HHI. A small p-value (¡ 0.05) determines that the null hypothesis is not supported, therefore supporting the hypothesis that HHI and the current HRI interactions (without shared control) are significantly different experiences for the local user.

Vigor/Energy: HRI handshakes have significantly lower acceleration waveform amplitudes compared to HHI handshakes ($p < 0.01$) . Waveform amplitude is measured from the y-axis waveform because the amplitude of the y-axis waveform is the most prominent and consistent of the three axes. Human-human acceleration amplitude is $3.9 \pm 0.16g$ and human-robot acceleration amplitude is $1.3 \pm 0.43g$.

Duration: HHI handshakes are significantly quicker than HRI handshakes ($p < 0.01$). Human-human handshake duration is $1.1 \pm 0.40seconds$ while human-robot duration is $3.1 \pm 0.73seconds$ showing a significant increase in duration for human-robot handshakes. It is worth noting that the duration of handshakes determined by FSR contact is consistent with the duration determined by the accelerometer.

Pulses: HRI handshakes have significantly more pulses ($p < 0.01$) compared to HHI handshakes. Waveform peaks are counted in stage 3 of each handshake from the y-axis of the acceleration data because it is the most prominent and consistent. The average number of human-human waveform peaks is $3.6 \pm 1.6peaks$ while the average number of human-robot waveform peaks is $6.7 \pm 1.5peaks$.

Firmness/Grip Strength: HRI handshakes have significantly lower firmness ($p = 0.047$) compared to HHI handshakes as determined by average voltages of activated FSRs. Firmness is determined by taking the mean of the magnitude of force (N) applied to the sensors that are activated in each trial (ignoring the sensors that are not activated so the data is not biased by differences in grip completeness). The mean force exerted on FSRs during human-human trials is $10.5 \pm 8.54N$ while the mean force for human-robot trials is $6.02 \pm 7.62N$.

Completeness of Grip: The number of FSRs activated in HRI handshakes is significantly lower than HHI handshakes ($p < 0.01$), suggesting a lesser completeness of grip. To determine completeness, the number of sensors activated for each trial is counted. The average sensor activation per human-human handshake (out of 5) is $3.3 \pm 0.75sensors$. The average per human-robot handshake is $2.1 \pm 1.0sensors$.

C. Additional Results

Gyroscope data displays five distinct regions of both human-human and human-robot interactions that matches the five regions displayed by the accelerometer data. The data it provides in relation to the 5 handshake characteristics (vigor, firmness, completeness of grip, number of pulses, and duration) is consistent with accelerometer data and therefore redundant. However, trends from gyroscope data are important to note because common rotations during each handshake stage may be useful in creating an average predisposed handshake movement profile for the robot to follow in shared control implementation. Notable trends include relatively constant rotation around the z-axis during stage 1 and 5, a single spike in angular velocity around the x-axis in stages 2 and 4 with large data variations for the y-axis and z-axis, and a low amplitude waveform in stage 3. For human-robot interactions, the z-axis is included in the waveform with the same phase and similar magnitude as the x-axis.

Magnetometer data is not presented in detail because no unique data is provided from it. The magnetometer, which measures the magnetic pull experienced along each axis in relation to magnetic north, shows orientation changes. The orientation of the hand during a handshake only changes significantly when the hand is raised and lowered in stages 1 and 5.

VII. Discussion

The results of the user study demonstrate the capability of the HMG to quantify differences between HHI and HRI handshakes with the current telerobotic system. They also illuminate necessary improvements to the system such as

providing haptic feedback to the remote user to enable bilateral responses. Another necessary improvement is implementing shared control within the system by using active data from the HMG to allow the telerobot to automatically adjust to the natural handshake of the local user.

A. Handshake Stages Discussion

Stages 2, 3, and 4 represent the core functions of the handshake, containing the most complex and variable interactions. Similar to observations made in [18], stage 2 exhibits varying data trends across all sensors. Data is inconsistent during stage 2 because every person has a unique predisposed expectation of the handshake. Stage 2 for a human involves using natural haptic feedback capabilities to actively adapt a unique handshake style to another's handshake style. Consequently, acceleration, grip (strength and completeness), and rotation change until a medium is reached between the two objects. We hypothesize that a haptic interface for the remote user would help in stage 2 of HRI handshakes by allowing the remote user to respond to the local user's handshake style. During stage 3, completeness of grip and firmness are constant while vigor and pulses are steadily periodic. Here again, however, we observe that HRI handshakes are slower and have more waveform periods, likely due to the local user compromising to the remote user's movement. Stage 4 follows a similar explanation as stage 2. The data from all sensors is highly varied because each person has a unique expectation of when the handshake should end. For example, as shown in stage 4 of Fig. 6 (b), the participant decided the handshake was done and slowed the motion but restarted the motion when they received feedback to continue from the robot. However, there are some noticeable trends in stage 4 such as a decrease in grip force, decrease in linear acceleration waveform amplitudes, and decrease in angular velocities as motion slows down before release, which could be useful in future work with remote haptic feedback and shared control for informing when the handshake should end.

B. Handshake Metrics Discussion

In almost every category, the HRI handshake was significantly different than the HHI handshake. While this is expected, the data presented here makes the strong case for the need of a shared control algorithm in executing social contact interactions as well as haptic feedback for the remote user if these interactions are to be natural. These metrics also illustrate technical improvements that can be made to the current robot system. For example, the FSR data provided a significantly lower completeness of grip for HRI with 2.1/5 sensors activated per handshake compared to 3.3/5 sensors for HHI. Part of this difference can be explained by the nuance of shaking hands with a robot. It was qualitatively observed that participants were hesitant to fully grasp the robot hand, as if they may break it. Additionally, the HMG has less surface contact with the Brunel Hand 2.0 than it does with a human hand due to its shape and actuation, a limitation which attributes to the lower HRI completeness of grip. The FSR data showed a decrease in grip firmness between HHI (10.5 N) and HRI (6.02 N). Participants lowered their firmness, perhaps in fear of damaging the robot. As reported by one participant, "I was cautious in the beginning because I did not want to damage [the robot]. I definitely felt force in the right areas from the robot and a certain amount of grip, but not a firm grip." On the robot end, the fingers often did not fully grip participant hands because of resolution discrepancies in finger movement tracking with the Manus VR glove. This results in a lower firmness from the robot hand. The lower vigor of HRI with waveform amplitude 1.3g compared to HHI (3.9g amplitude) is a product of the participant's hesitation to shake the robot hand confidently and the remote user's inability to determine the actual vigor the robot outputs based on tracking. We hypothesize that the lack of rich touch information on the remote user side is also reason for the longer duration of HRI (3.1s) compared to HHI (1.1s) handshakes.

VIII. Conclusion and Future Work

This work presents the design of a wireless HMG for sensing in social contact interactions and presents a comparative user study analyzing handshakes in HHI and HRI settings. Results demonstrated differences in HHI and HRI handshakes in each area studied as expected. The HMGs were capable of accurately and consistently recording all desired parameters (firmness, vigor, duration, completeness of grip, and number of pulses) as well as characterize five stages of handshakes. The low profile hardware on the HMGs with their wireless design allowed uninterrupted interactions, so all defined constraints were satisfied. One improvement that is being considered in a future design of the HMG is time-stamping capabilities. A constant time stamp between the two gloves would allow linking data from both ends of an interaction to evaluate how one participant reacted to another. Data linking would require wireless communication between the gloves either through Bluetooth moduli or transceivers.

A. Shared Control and Haptic Feedback

The findings from this work, taken together, detail the complexities of social, contact interactions and illustrate the challenges of executing these appropriately and naturally over telerobotic platforms. We hypothesize that a shared control architecture would alleviate some of the challenges in executing these interactions. Our vision for shared control in this context is that the remote user would initiate a desired interaction (such as a handshake) via a natural gesture (such as sticking one's hand out in a shaking pose), at which point the telerobot would take over control of the manipulator to complete the interaction. To do this, the data sensed by the HMG would be transmitted live to the central processor of the telerobot. FSR data could provide live information about firmness and completeness of grip while the accelerometer would transmit vigor and pulse data. The processor would actively analyze the live HMG data stage-by-stage in comparison to a standard set of human-human data. The shared control system would then edit the manipulator actuation with the goal of achieving an HRI handshake with firmness,

completion of grip, vigor, number of pulses, and duration similar to that of a HHI handshake. We believe this would improve performance of the interaction, as well as alleviate the workload (both physical and cognitive) that currently exists with the remote user.

We hypothesize haptic feedback for the remote user is another way to create a more natural HRI handshake by allowing bilateral force adaptation similar to the experience of HHI handshakes. Haptic feedback would expand on the current solely visual feedback provided to the remote user and enable more organic information processing. Our view for this includes actuation hardware built into the Manus VR glove such as a flexible linear actuator band around the hand to simulate grip information from the FSRs, and vibrational or servo motors on the sides of the hand to relay pulse and vigor information from the IMU Such an implementation could improve the execution of social contact interactions by allowing the remote user to process and react to non-visual information from the local user. Future work will focus on the incorporation of haptic feedback for the remote user coupled with shared control architectures to alleviate the workload associated with executing complex interactions in telerobotic communication, while also making such interactions more natural.

ACKNOWLEDGMENT

This work is supported by the National Science Foundation under Grant No.s 1618926 and 1618283. Any opinions, findings and conclusions or recommendations expressed in this material are those of the author(s) and do not necessarily reflect the views of the National Science Foundation.

REFERENCES

[1] M. K. Lee and L. Takayama, ""now, I Have a Body": Uses and social norms for mobile remote presence in the workplace," in *Proceedings of the SIGCHI Conference on Human Factors in Computing Systems*, ser. CHI '11. New York, NY, USA: ACM, 2011, pp. 33–42.

[2] K. Tanaka, H. Nakanishi, and H. Ishiguro, "Robot conferencing: Physically embodied motions enhance social telepresence," in *CHI '14 Extended Abstracts on Human Factors in Computing Systems*, ser. CHI EA '14. New York, NY, USA: ACM, 2014, pp. 1591–1596.

[3] ——, "Physical embodiment can produce robot operators pseudo presence," *Frontiers in ICT*, vol. 2, 2015.

[4] D. Sakamoto, T. Kanda, T. Ono, H. Ishiguro, and N. Hagita, "Android as a telecommunication medium with a human-like presence," in *2nd ACM/IEEE International Conference on Human-Robot Interaction (HRI)*. IEEE, March 2007, pp. 193–200.

[5] E. Dreyfuss. (2015, Sept.) My Life as a Robot. [Online]. Available: https://www.wired.com/2015/09/my-life-as-a-robot-double-robotics-telecommuting-longread/

[6] H. Nakanishi, K. Tanaka, and Y. Wada, "Remote handshaking: Touch enhances video-mediated social telepresence," in *Proceedings of the SIGCHI Conference on Human Factors in Computing Systems*, ser. CHI '14. New York, NY, USA: ACM, 2014, pp. 2143–2152.

[7] V. A. Newhart, "Virtual inclusion via telepresence robots in the classroom," in *CHI 14 Extended Abstracts on Human Factors in Computing Systems*, ser. CHI EA 14. New York, NY, USA: Association for Computing Machinery, 2014, p. 951956.

[8] F. Tanaka, A. Cicourel, and J. R. Movellan, "Socialization between toddlers and robots at an early childhood education center," *Proceedings of the National Academy of Sciences*, vol. 104, no. 46, pp. 17 954–17 958, 2007.

[9] C. Stahl, D. Anastasiou, and T. Latour, "Social telepresence robots: The role of gesture for collaboration over a distance," in *Proceedings of the 11th PErvasive Technologies Related to Assistive Environments Conference*, ser. PETRA 18. New York, NY, USA: Association for Computing Machinery, 2018, p. 409414. [Online]. Available: https://doi.org/10.1145/3197768.3203180

[10] J. T. Slack, K. DeProw, Z. Anderson, R. M. Albacete Di Bartolomeo, J. B. Weinberg, and J. L. Gorlewicz, "Design of a lightweight, ergonomic manipulator for enabling expressive gesturing in telepresence robots," in *2018 IEEE/RSJ International Conference on Intelligent Robots and Systems*, ser. IROS. IEEE, 2018, pp. 5491–5496.

[11] K. M. Tsui, M. Desai, H. A. Yanco, and C. Uhlik, "Exploring use cases for telepresence robots," in *Proceedings of the 6th International Conference on Human-robot Interaction*, ser. HRI '11. New York, NY, USA: ACM, 2011, pp. 11–18.

[12] M. J. Hertenstein, D. Keltner, B. App, B. A. Bulleit, and A. R. Jaskolka, "Touch communicates distinct emotions," *Emotion*, vol. 6, no. 3, pp. 528–533, 2006.

[13] M. J. Hertenstein, R. Holmes, M. McCullough, and D. Keltner, "The communication of emotion via touch," *Emotion*, vol. 9, no. 4, pp. 566–573, 2009.

[14] B. App, D. N. McIntosh, C. L. Reed, and M. J. Hertenstein, "Nonverbal channel use in communication of emotion: How may depend on why," *Emotion*, vol. 11, no. 3, pp. 603–617, 2011.

[15] H. A. Samani, R. Parsani, L. T. Rodriguez, E. Saadatian, K. H. Dissanayake, and A. D. Cheok, "Kissenger: Design of a kiss transmission device," in *Proceedings of the Designing Interactive Systems Conference*, ser. DIS 12. New York, NY, USA: Association for Computing Machinery, 2012, p. 4857.

[16] R. Wang, F. Quek, D. Tatar, K. S. Teh, and A. Cheok, "Keep in touch: Channel, expectation and experience," in *Proceedings of the SIGCHI Conference on Human Factors in Computing Systems*, ser. CHI '12. New York, NY, USA: ACM, 2012, pp. 139–148.

[17] W. F. Chaplin, J. B. Phillips, J. D. Brown, N. R. Clanton, and J. L. Stein, "Handshaking, gender, personality, and first impressions," *Journal of Personality and Social Psychology*, vol. 79, no. 1, 2000.

[18] A. Melnyk, P. Henaff, V. Khomenko, and V. Borysenko, "Sensor network architecture to measure characteristics of a handshake between humans," in *2014 IEEE 34th International Scientific Conference on Electronics and Nanotechnology (ELNANO)*. IEEE, 2014, pp. 264–268.

[19] Z. Wang, J. Hoelldampf, and M. Buss, "Design and performance of a haptic data acquisition glove," in *Proceedings of the 10th Annual International Workshop on Presence*, 2007, pp. 349–357.

[20] S. Wiley, T. Blackwell, D. Casner, and B. Holson, "Self-balancing robot having a shaft-mounted head," U.S. Patent 8 306 664B1, Nov. 6, 2012.

[21] W.-C. Chang, M.-Y. Tseng, and N.-J. Cheng, "Virtual reality system and method for controlling operation modes of virtual reality system," U.S. Patent 9 952 652B2, Apr. 24, 2018.

[22] Y.-C. Huang, W.-H. Shih, H.-Y. Tseng, C.-T. Chen, C.-W. Chang, S.-C. Tsai, and Y.-C. Lin, "Wireless control device, position calibrator and accessory," U.S. Patent 10 162 414B2, Dec. 25, 2018.

[23] (2017) Prime One Gloves—Manus VR. [Online]. Available: https://manus-vr.com/prime-one-gloves/

[24] "Mpu-9250 product specification revision 1.0," InvenSense, San Jose, CA, USA.

[25] "Force sensing resistor integration guide and evaluation parts catalog," Interlink Electronics, Camarillo, CA, USA.

[26] Z. Anderson, E. Capelle, W. Benson, J. Gorlewicz, and J. Weinberg, "Video comparison of hhi and hri handshakes." [Online]. Available: https://sites.google.com/slu.edu/gorlewicz-lab/research/enhancing-teleoperative-systems